

STRATOSPHERIC AEROSOL OBSERVATIONS FOLLOWING THE ERUPTION  
OF EL CHICHON

G. S. Kent

Science and Technology Corporation  
Hampton, Virginia 23661

M. P. McCormick  
NASA-Langley Research Center  
Hampton, Virginia 23665

ABSTRACT

Several eruptions of the El Chichon volcano between March 28 and April 4, 1982 produced a global enhancement of the stratospheric aerosol content which seriously affected satellite measurements of properties of the earth and its atmosphere. This enhancement, possibly the largest in the past seventy years, has since been monitored by in situ, as well as, satellite and ground-based remote sensing techniques. The injected material, at latitude 17°N and at altitudes up to 30 km, spread rapidly zonally and more slowly meridionally. Airborne lidar measurements showed that the maximum global mass loading of about  $1.2 \times 10^7$  tonnes occurred 3-6 months after the eruptions. By May 1983, the aerosol was well distributed globally, with peak concentrations within a rather broad equatorial band and between 40° and 60°N and S. The altitude of the peak aerosol mixing ratio, initially at about 27 km in the equatorial zone, had decreased by 5-6 km by May 1983. Midlatitude lidar measurements showed a similar decrease, accompanied by loss of material from the stratosphere into the troposphere. Estimates of the 1/e decay time for the aerosol mass loading vary between 5 and 14 months, depending upon latitude and measurement techniques, with a northern hemisphere average of about 10 months.

INTRODUCTION AND BACKGROUND

(a) The Eruption of El Chichon

The El Chichon volcano is situated in Mexico at latitude 17.3°N and longitude 93.2°W. Four major eruptions took place between 28 March 1982 and 4 April 1982 when the final and largest explosion occurred. GOES and NOAA-6 satellite observations of the clouds from these eruptions indicated that at least two and possibly three of the eruptions penetrated the tropopause (BANDEEN and FRASER, 1982). The cloud quickly spread westward over the Pacific Ocean and lidar observations made at the Mauna Loa Observatory in Hawaii on 9 April 1982 showed a scattering layer at an altitude of 26 km, the scattering ratios being the greatest ever observed there (DeLUISI et al., 1983). Subsequent lidar (McCORMICK et al., 1984) and in situ balloon measurements (HOFMANN and ROSEN, 1983a) showed that the injected material extended up to an altitude of about 30 km and that there appeared to be two layers separated by a region of minimum concentration at an altitude of about 21 km, possibly associated with separate eruptions of the volcano or different wind regimes.

Perturbing effects of the stratospheric cloud quickly became apparent on several satellite systems and these perturbations provided a useful means with which to map the spreading of the cloud. Notable among these were the effects on the Nimbus 7 Total Ozone Mapping Spectrometer (KRUEGER, 1983), the Solar Mesospheric Explorer (BARTH et al., 1983) and the AVHRR sea surface temperature sensor (STRONG, 1984).

NASA-17959

7N 46-12  
27086

MAA/TIS

1988 FEB 11 A 8:21

N90-70578

Unclass  
0270860  
00/46

(NASA-TM-102893) STRATOSPHERIC AEROSOL  
OBSERVATIONS FOLLOWING THE ERUPTION OF EL  
CHICHON (NASA) 12 P

## (b) Typical Behavior of Volcanic Stratospheric Aerosol

Several volcanic eruptions in the previous five years have injected material into the stratosphere although none has been the magnitude of El Chichon. The behavior of the stratospheric clouds formed has been sufficiently well documented by remote and in-situ measurement techniques that it is possible to describe a typical scenario. The initial volcanic column consists of a mixture of ash particles, water vapor and sulphurous gases (DEEPAK, 1982). This expands and is dispersed by high altitude winds which are predominantly of a zonal nature and sharp concentration gradients are formed by the action of wind shears. In the days following the eruption, sedimentation of the larger ash particles takes place and sulphuric acid is produced by chemical transformation of the sulphur dioxide in the cloud (TURCO et al., 1982). The sulphuric acid nucleates to form new aerosol particles and condenses onto preexisting aerosol particles. This gas to particle conversion process causes the mass of aerosol resulting from the cloud to rise to a maximum 3-6 months after the eruption. At the same time, the material is dispersed globally with major inhomogeneities in concentration which slowly disappear. Global dispersion is a function of volcanic latitude and, to a certain extent, of season of eruption. The injected material from high latitude eruptions tends to remain within that hemisphere, material from low latitude eruptions spreads into both hemispheres forming zonal concentrations near the equator and at high northern and southern latitudes. Following the time of maximum aerosol loading, a slow decay is observed due to particle loss into the troposphere. This has a  $1/e$  decay time constant of 6-12 months. Although the El Chichon eruption was on a larger scale than other recent eruptions, there was no reason to believe that its behavior should be radically different. An unknown factor was the likely effect of the rather high injection altitudes (layer peak at ~26 km) as compared to these earlier eruptions.

## (c) Methods of Observation

The El Chichon volcano has been the subject of considerable scientific study, often in the form of coordinated missions. Table 1 shows a list of some of the main techniques used for study; neither the list nor the references given are intended to be exhaustive, but to illustrate the range of measurements made. The early period, just after the eruptions, is the most intensively studied, as is appropriate for a period of rapid change and still relatively unknown behavior. Routine measurements of the aerosol cloud characteristics both by remote and in-situ techniques have nevertheless continued to the present time.

## CLOUD CHARACTERISTICS AND BEHAVIOR, APRIL-DECEMBER, 1982

### (a) Global Dispersion

The early stages of the spreading of the stratospheric dust cloud are most clearly shown on the imaging from the NOAA-7, GOES-E and GOES-W satellite (ROBOCK and MATSON, 1983). This showed the cloud to have spread westward from Mexico in a narrow zonal band which circumnavigated the globe by 25 April 1982. The band passed over Mauna Loa, Hawaii, where lidar observations showed backscattering ratios of over 300, the densest part of the cloud being at about 27 km with an upper boundary at 35 km (DeLUISI et al., 1983). Optical depth values at 425 nm reached 0.7 in April, 1982, as compared to a normal background value of 0.02.

TABLE 1. OBSERVATIONAL METHODS USED TO STUDY THE STRATOSPHERIC EFFECTS OF THE EL CHICHON VOLCANIC ERUPTION

<u>Technique</u>	<u>Notes</u>	<u>References</u>
<u>Ground-Based</u>		
Lidar backscatter	Numerous stations, mainly in the northern hemisphere.	McCormick, 1985; Jager et al., 1984; DeLuisi et al., 1983; Reiter et al., 1983; Adriani et al., 1983; Post, 1985; Uchino, 1985; Clemesha & Simonich, 1983; Shibata et al., 1984.
Sun photometer optical depth	Part of long-term data set from Mauna Loa, Hawaii.	DeLuisi et al., 1983.
Spectrophotometer SO <sub>2</sub> measurements	Used to estimate total SO <sub>2</sub> injection.	Evans and Kerr, 1983.
<u>Airborne and Balloon</u>		
Lidar backscatter	Numerous flights by NASA-LaRC.	McCormick & Swisler, 1983; McCormick et al., 1984.
In-situ sampling of aerosol size and composition	Aircraft flight altitude limits sampling to lower part of aerosol cloud.	Oberbeck et al., 1983; Knollenberg & Huffman, 1983; Gooding et al., 1983; Gandrud et al., 1983; Woods & Chuan, 1983; Mroz et al., 1983.
In-situ gaseous sampling or over-burden measurement	Aircraft flight altitude limits sampling to lower part of aerosol cloud.	Vedder et al., 1983; Evans & Kerr, 1983.
Balloon-based particle counter	Numerous flights to 30 km by U. of Wyoming.	Hofmann & Rosen, 1983ab; Hofmann & Rosen, 1984.
Infra-red transmission	Additional absorption features due to El Chichon effluents measured.	Witteborn, et al., 1983.
Multi-wavelength sun photometer	Measures wavelength dependence of optical depth.	Dutton & DeLuisi, 1983; Swisler et al., 1983; Spinhirne, 1983.
<u>Satellite</u>		
Nimbus 7 - TOMS	Shorter wavelengths used to map SO <sub>2</sub> cloud.	Krueger, 1983.
NOAA 7 & GOES	Mapped spreading of dust cloud.	Robock & Matson, 1983.
SME thermal emission	Mapped initial distribution of aerosol cloud.	Barth et al., 1984; Thomas et al., 1983.
AVHRR	Negative bias on sea surface temperature indicated location of aerosol cloud.	Strong, 1984.
SAM II	1 $\mu$ m optical depth in polar regions only.	McCormick, 1985.
SAGE II	Since October 1984 only.	Mauldin et al., 1985.

Meridional spreading of the cloud was observed by lidar in middle and high latitudes. At Tsukuba in Japan 30°N, 140°E a new aerosol layer, at an altitude of 15 km, was seen on 25 April 1982 (UCHINO, 1985) and at Langley, USA (37°N, 76°W) a layer at a similar altitude was seen on 29 April (McCORMICK et al., 1984). This low altitude cloud reached European lidar stations soon afterwards. It was observed over Frascati, Italy (42°N, 23°E) on 13 May 1982 (ADRIANI et al., 1983) and over Garmisch-Partenkirchen (47°N, 11°E) on 3 May 1982 (REITER et al., 1983). Movement of the cloud into the southern hemisphere proceeded more slowly; lidar observations at San Jose dos Campos (23°S, 40°W) showed the first major enhancement in July, 1982, peak scattering occurring, as in the northern hemisphere, at an altitude below 20 km (CLEMESHA and SIMONICH, 1983). These lidar observations are supported by satellite measurements. Data from SME, at a wavelength of 6.8  $\mu$ m, taken on May 21, 1982 showed the bulk of the injected material to lie between the equator and 30°N with a fringe of lower altitude material extending northwards to about 60°N (BARTH et al., 1983). Part of the material had even reached higher northern latitudes by this time. Examination of SAM II data (approximately 65°N-80°N) shows material below 20 km in altitude arriving there in May 1982.

A more accurate description of the meridional and altitudinal distribution of the material was obtained using the NASA/LARC airborne ruby lidar system on a flight between NASA Wallops Flight Center and the Caribbean between July 9-12, 1982. Individual vertical profiles showed a layer peak at an altitude of 26-27 km with maximum scattering ratios of about 50. Figure 1 shows contours of the aerosol backscatter ratio for the two flight directions. It is clear that the main layer above 21 km is still basically confined to the latitude band south of 25°N although material below 20 km has spread farther north.

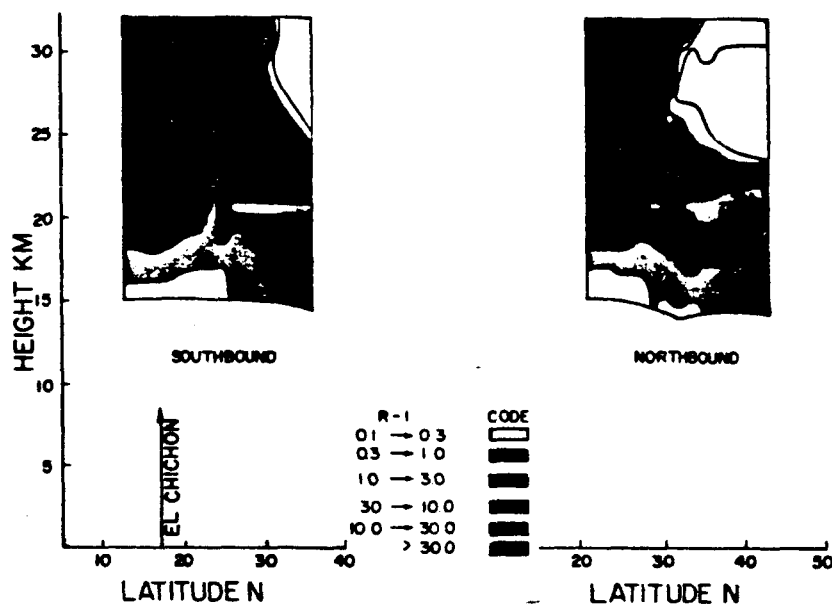


Figure 1. Contours of aerosol backscatter ratio (R-1) at  $\lambda = 0.6943 \mu\text{m}$  versus altitude and latitude for the July 9-12, 1982 flight campaign. (McCormick et al., 1984.)

Spreading of the higher altitude material was, in fact, noted by mid-latitude lidar stations in June 1982 and continued throughout the summer. During succeeding months, the vertical structure blurred, sharp layers disappearing and by the end of 1982, the distinction between upper and lower layers had largely disappeared. A second airborne lidar expedition in October 1982, which covered the latitude range 46°N-46°S showed aerosol dispersed over this entire latitude span, maximum concentrations were still, however, in a band between 10°S and 30°N (McCORMICK et al., 1984; McCORMICK and SWISSLER, 1983). Peak scattering ratios within this band occurred at the somewhat lower altitude of 24 km with a remarkable degree of zonal homogeneity. Figure 2 shows a set of lidar scattering profiles obtained at 19°N between longitudes 78°W and 86°W, where there is very little variation in aerosol distribution. SAM II data for the antarctic region obtained in December 1982 showed that the volcanic aerosol had reached high southern latitudes (65°S-80°S) by about this time. In the arctic region at this time, 1  $\mu\text{m}$  optical depth values were close to their peak levels of approximately 0.1 (weekly average value).

#### (b) Gaseous and Particle Characteristics

Estimates of  $\text{SO}_2$  concentrations have been made by satellite (KRUEGER, 1983), in-situ aircraft (VEDDER et al., 1983) and ground-based (EVANS and KERR, 1983) observations. These show that the  $\text{SO}_2$  cloud spread westward from Mexico with the aerosol cloud. An estimate of the quantity of  $\text{SO}_2$  deposited into the

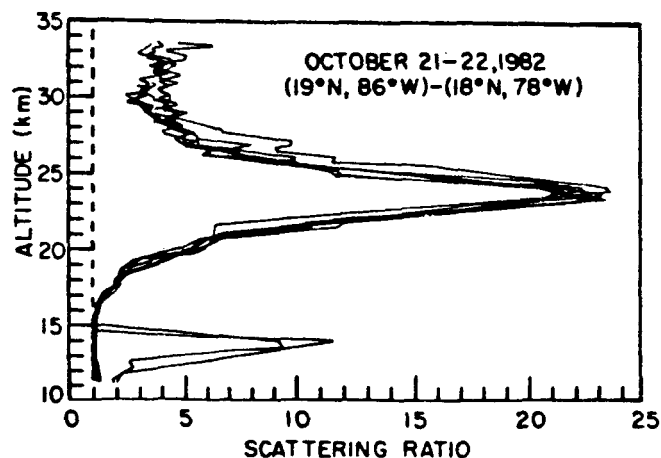


Figure 2. Vertical profiles of lidar scattering ratio between Mexico and Puerto Rico on October 21-22, 1982. The lower altitude (13-14 km) enhancement is a tropospheric cloud. (McCormick and Swissler, 1983.)

stratosphere by El Chichon, based on satellite measurements, is approximately  $3 \times 10^6$  tons. Mixing ratios from in-situ measurements in the lower part of the cloud during 1982 varied between 8 and 132 pptv. Ground-based measurements of  $\text{SO}_2$  column content in Mauna Loa have been used, in combination with airborne measurements, to arrive at a figure of approximately  $13 \times 10^6$  tons of  $\text{SO}_2$  injected. Airborne  $\text{SO}_2$  overburden measurements and independent sulphate mixing ratio measurements (MROZ et al., 1983) showed a latitudinal distribution similar to that measured optically for the plume.

Size-specific composition measurements on aerosols in the lower part of cloud using a quartz crystal microbalance (WOODS and CHUAN, 1983) showed a very complex situation. During the first months after the eruption, the aerosol mass was dominated by solid micrometer-sized particles. The submicrometer particles consisted largely of sulphuric acid. By November and December, 1982, fewer very large particles were evident, presumably having been removed by sedimentation. Similar results were obtained by GOODING et al. (1983) from flight samples collected at altitudes up to 19 km and between latitudes of  $10^\circ\text{S}$  and  $75^\circ\text{N}$ . These flights showed progressively finer grained ash samples with increasing time after the eruption. Samples collected in October 1982 were dominated by liquid droplets, assumed to be sulphuric acid.

Numerous aerosol size distribution and concentration measurements were made using balloon-borne particle counters at Laramie ( $41^\circ\text{N}$ ) and in southern Texas ( $27^\circ$ - $29^\circ\text{N}$ ) during the months following the El Chichon eruption (HOFMANN and ROSEN, 1983a,b, 1984). These have shown in some detail the variation of particle concentration and mass mixing ratio to altitudes of about 30 km. The measurements also confirm the formation of two major layers separated by a relatively clear region at an altitude of about 21 km. The aerosol mean radius in both layers grew with time, that in the upper layer peaking at around  $0.3 \mu\text{m}$ , approximately four months after the eruption and the mean radius in the lower layer rising more slowly to about  $0.2 \mu\text{m}$  one year after the eruption. The particle size distribution in the upper layer was initially bimodal with modes near  $0.02 \mu\text{m}$  and  $0.7 \mu\text{m}$ . This is consistent with simultaneous nucleation from gaseous  $\text{H}_2\text{SO}_4$  and growth of preexisting aerosols. The reasons for the behavioral differences at 18 and 25 km are not clear but may be connected with

the more rapid global dispersion of the 18 km layer or in the production of the layers by different explosions.

### (c) Mass Loading

Some estimates of the mass of injected  $\text{SO}_2$  gas have already been quoted and ROSEN and HOFMANN (1983a) estimated an injection mass of  $8\text{--}20 \times 10^6$  tonnes, depending upon time after the eruption. McCORMICK and SWISSLER (1983, 1985) have combined data from the series of NASA-LaRC lidar flights and SAM II optical depth measurements to not only estimate the peak aerosol mass loading but also to study its decay. The time from the eruption of El Chichon to apparent peak stratospheric loading was observed to vary with altitude from 3–4 months in the latitude belt close to El Chichon to about one year at high northern latitudes. Viewed more globally, the mass probably peaked between August and September, 1982 (McCORMICK, 1984). Individual lidar flights have been used to calculate the integrated aerosol backscatter from the tropopause upwards as a function of latitude. This is shown in Fig. 3 for the flight of October–November, 1982 (McCORMICK and SWISSLER, 1983).

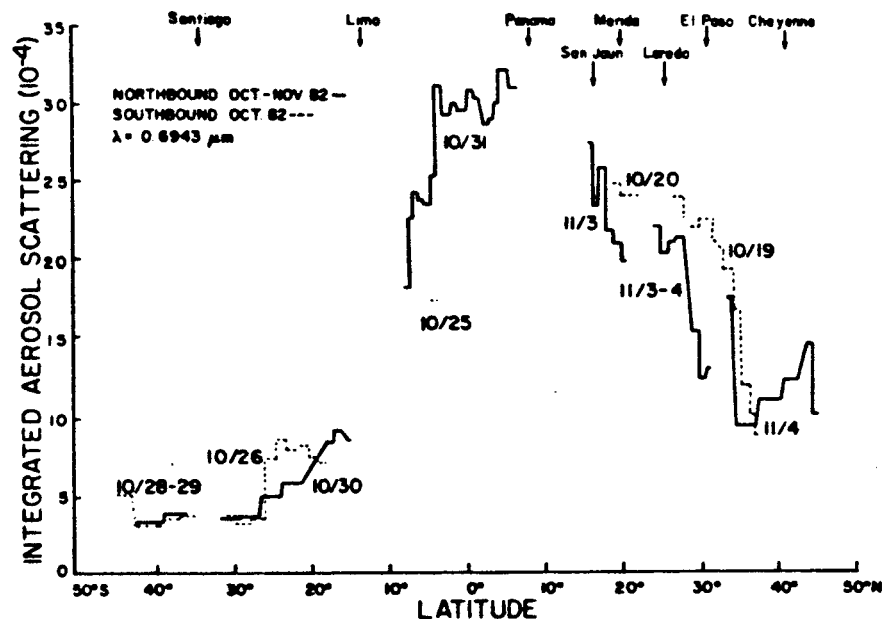


Figure 3. Integrated aerosol backscattering function from the tropopause through the stratospheric layer versus latitude for the southbound and northbound flights. (McCormick and Swisler, 1983.)

Conversion to aerosol mass loading involves the use of a model for aerosol particle size distribution and composition. In this case, the model used is based on the University of Wyoming's six-channel balloon-borne particle counter data from Del Rio, Texas, also for October, 1982. Total aerosol mass loading calculated in this way was  $11.0 \times 10^6$  tonnes. Allowing for the aerosol loading outside the latitude limits of the lidar flight (based on SAM II data), and subtracting the preexisting aerosol a total of  $12 \times 10^6$  tonnes is arrived at for the global total from El Chichon. Confidence in this value is increased by the results of a comparison of the lidar derived, wavelength dependent, optical depth with direct sun photometer measurements (SWISSLER et al., 1983) taken on the same flight. Good agreement was found between the two data sets confirming

the reasonableness of the optical model used with the lidar data. Global stratospheric aerosol optical depth values during the time of maximum loading varied from 0.03 to 0.15 for visible wavelengths; highest values were observed about 20°N latitude (SPINHIRNE, 1983). Table 2 shows a list of estimated stratospheric aerosol masses injected by significant volcanic injection. The total aerosol from El Chichon is an order of magnitude greater than any other eruption during the previous ten years and is comparable to the stratospheric input from Agung and earlier massive eruptions.

TABLE 2. ESTIMATES OF AEROSOL MASS LOADING FROM VOLCANIC ERUPTIONS

		<u>Total Global Injection (10<sup>6</sup>Metric Tons)</u>	<u>Source</u>
August 1883	Krakatoa	50	Diermendjian (1973)
June 1912	Katmai	20	Diermendjian (1973)
March 1963	Agung	16	Diermendjian (1973)
		30	Cadle, et al. (1976, 1977)
October 1974	Fuego	6	Cadle, et al. (1976, 1977)
		3	Lazrus, et al. (1979)
1979	Background	0.57	Kent & McCormick (1984)
November 1979	Sierra Negra	0.16	Kent & McCormick (1984)
May 1980	St. Helens	0.55	Kent & McCormick (1984)
October 1980	Ulawun	0.18	Kent & McCormick (1984)
April 1981	Alaid	0.50	Kent & McCormick (1984)
May 1981	Pagan		
January 1982	Mystery Volcano	0.85	Mroz et al. (1983)
April 1982	El Chichon	12.0	McCormick (1984)

#### (d) Temperature Impact

An interesting aspect of the stratospheric influence of the El Chichon aerosol has been the effect on stratospheric temperature. LABITZKE et al. (1983) have shown that the 30 mb temperatures between 10°N and 30°N during July-October, 1982 were significantly warmer than in the same months in previous years. Temperature deviations were as high as 5°C, the maximum change coinciding in latitude, altitude and time with the peak aerosol concentrations. These findings are consistent with one-dimensional radiative-convective models which predict that the aerosols from a major eruption such as El Chichon or Agung will warm the stratosphere and cool the earth's surface (HANSEN et al., 1978).

#### CLOUD CHARACTERISTICS AND BEHAVIOR, 1983-1985

The years 1983-1985 have constituted a period during which the aerosol from the El Chichon eruption has been in a slow decay phase. The aerosol has spread relatively uniformly globally, with its main concentrations lying in three bands centered on the equator and high northern and southern latitudes, respectively. Figure 4 shows a perspective view of the integrated backscatter derived from five NASA-LaRC lidar flights between July, 1982 and January, 1984. The zonal structure is clearly visible in the data for May, 1983 and is similar to that seen for earlier eruptions (KENT and McCORMICK, 1984). At the same

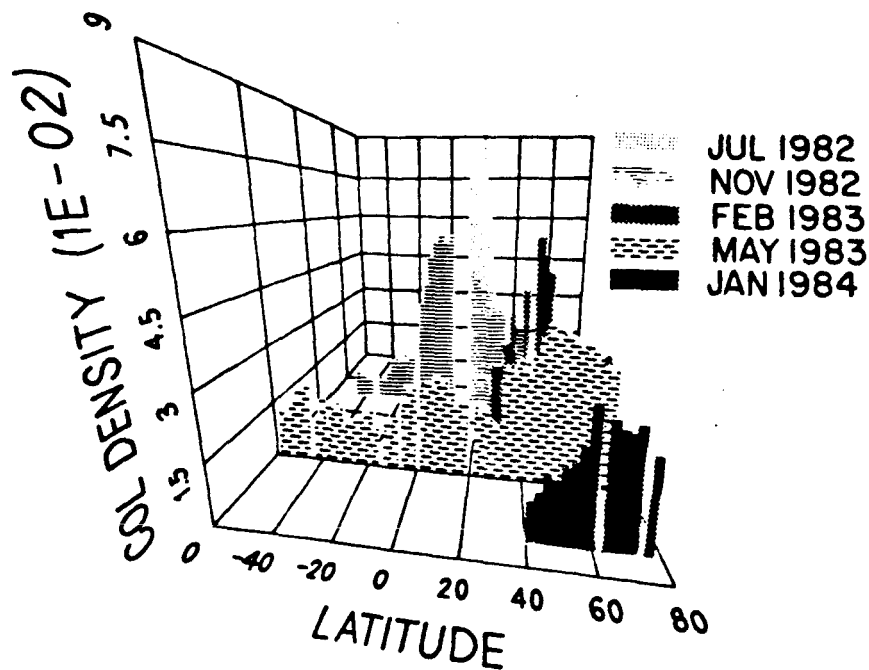


Figure 4. Perspective diagram showing integrated backscatter as a function of latitude for five airborne lidar missions between July 1982 and January 1984.

time, the integrated backscattering and extinction have been decreasing. This is shown in the mid-latitude lidar record (McCORMICK et al., 1984) and high latitude SAM II extinction data (McCORMICK and SWISSLER, 1985).  $1 \mu\text{m}$  peak aerosol extinction values, measured by the Stratospheric Aerosol and Gas Experiment II (SAGE II--MAULDIN et al., 1985) in November 1984, were about  $1.5 \times 10^{-3} \text{km}^{-1}$  in medium northern latitudes, or about one order of magnitude greater than the background value in 1979. The NASA-LaRC 48" lidar record shown in Fig. 5 recorded integrated backscatter values in the first half of 1985 about a factor of six above the 1979 levels. Recently, McCORMICK and SWISSLER (1985) have used lidar and satellite extinction data to estimate the decay rate for the aerosol mass loading. These decay rates were found to be dependent upon latitude and period of calculation. The average  $1/e$  time for the northern hemisphere and a time interval of a year or more was found to be 10-11 months. This period, and the period from the eruption to maximum stratospheric effect (3-6 months), are similar to those found for earlier eruptions.

At the same time that the aerosol optical effects have been decreasing, the mean aerosol radius in the upper part of the cloud has been decreasing (HOFMANN and ROSEN, 1984) and the altitude of the layer peak in the northern hemisphere decreased from about 26 km in August 1982 to about 21 km in August 1983 (McCORMICK, 1984). Backscatter measurements (POST, 1985) at  $10.6 \mu\text{m}$  and  $40^\circ\text{N}$  show a similar decrease of both peak backscattering and cloud altitude. The time constant for removal from the stratosphere was found by POST (1985) to be 208 days, in fair agreement with the value quoted earlier. In addition, the volcanic aerosol can be seen entering the upper troposphere where it had a shorter residence time of about 60 days. Similar stratospheric-tropospheric aerosol transfer was seen after the earlier eruption of Mt. St. Helens (KENT et al., 1985).



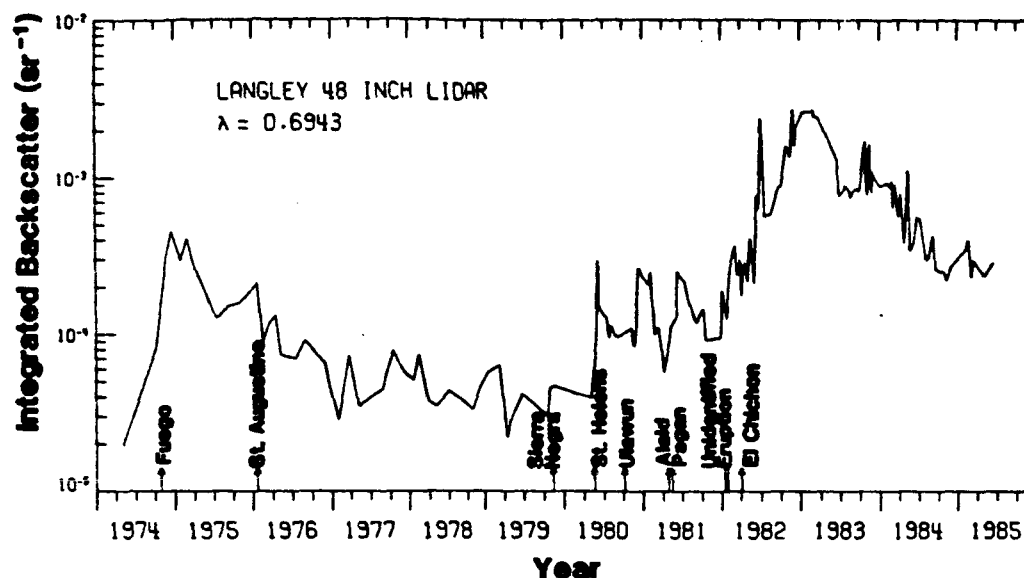


Figure 5. Long-term variation of integrated stratospheric aerosol backscattering function obtained at Hampton, Virginia (37°N).

#### CONCLUSIONS

The stratospheric effects of the El Chichon eruptions have been well surveyed by satellite, in-situ and ground-based remote sensors. These have shown that the stratospheric cloud, injected into the stratosphere at approximately 17°N, reached an altitude of at least 30 km. The cloud circled the globe in about 3 weeks and meridional transport of the lower level material was also observed in medium and high northern latitudes, using lidar, within a few weeks of the eruption. Movement of the upper part of the cloud, initially peaking at around 26 km, was somewhat slower, but by the end of 1982, the cloud was well dispersed globally. A maximum stratospheric loading of about  $1.2 \times 10^7$  tonnes was observed about 3-6 months after the eruption, making this one of the most significant eruptions of this century. Aerosol optical depth values, in the visible region of the spectrum at this time, were between 0.03 and 0.15. Average 1/e decay times for the concentration of the injected aerosol have been determined from satellite and lidar observations to be about 10 months.

#### ACKNOWLEDGMENTS

One of us (G.S.K.) is supported under NASA Contract NAS1-17959.

#### REFERENCES

- Adriani, A., F. Congeduti, G. Fiocco and G. P. Gobbi, One year lidar observations of the stratospheric aerosol at Frascati, March 1982-March 1983, Geophys. Res. Lett., **10**, 1005-1008.
- Bondeen, W. R. and R. S. Fraser, Radiative effects of the El Chichon volcanic eruption: Preliminary results concerning remote sensing, NASA Technical Memorandum 84959, 1982.

- Barth, C. A., R. W. Sanders, R. J. Thomas, B. M. Jakosky and R. A. West, Formation of the El Chichon aerosol cloud, Geophys. Res. Lett., 10, 993-996, 1983.
- Cadle, R. D., C. S. Kiang, and J. F. Louis, The global scale dispersion of the eruption clouds from major volcanic eruptions, J. Geophys. Res., 81, 3125-3132, 1976.
- Cadle, R. D., F. G. Fernald, and C. L. Frush, Combined use of lidar and numerical diffusion models to estimate the quantity and dispersion of volcanic eruption clouds in the stratosphere: Volcan Fuego, 1974, and Augustine, 1976, J. Geophys. Res., 82, 1783-1786, 1977.
- Clemesha, B. R. and D. M. Simonich, Lidar observations of the El Chichon dust cloud at 23. S, Geophys. Res. Lett., 10, 321-324, 1983.
- Deepak, A. (Ed.), Atmospheric effects and potential climatic impact of the 1980 eruptions of Mount St. Helens, NASA Conference Publication 2240, 1982.
- Deirmendjian, D., On volcanic and other particulate turbidity anomalies, Advan. Geophys., 16, 267-296, 1973.
- DeLuisi, J. J., E. G. Dutton, K. L. Coulson, T. E. DeFoor, and B.G. Mendonca, On some radiative features of the El Chichon volcanic stratospheric dust cloud and a cloud of unknown origin observed at Mauna Loa, J. Geophys. Res., 88, 6769-6772, 1983.
- Dutton, E. G. and J. DeLuisi, Spectral extinction of direct solar radiation by the El Chichon cloud during December 1982, Geophys. Res. Lett., 10, 1013-1016, 1983.
- Evans, W. E. I. and J. B. Kerr, Estimates of the amount of sulphur dioxide injected into the stratosphere by the explosive volcanic eruptions: El Chichon, mystery volcano, Mt. St. Helens, Geophys. Res. Lett., 10, 1049-1051, 1983.
- Gandrud, B. W., M. A. Kritz, A. L. Lazrus, Balloon and aircraft measurements of stratospheric sulphate mixing ratio following the El Chichon eruption, Geophys. Res. Lett., 10, 1037-1040, 1983.
- Gooding, J. L., D. S. Clanton, E. M. Gabel, and J. L. Warren, El Chichon volcanic ash in the stratosphere: Particle abundance and size distribution after the 1982 eruption, Geophys. Res. Lett., 10, 1033-1036, 1983.
- Hansen, J. E., W. Wang, and A. A. Lacis, Mount Agung eruption provides test of a global climatic perturbation, Science, 199, 1065-1068, 1978.
- Hofmann, D. J. and J. M. Rosen, Sulfuric acid droplet formation and growth in the stratosphere after the 1982 eruption of El Chichon, Science, 22, 325-327, 1983a.
- Hofmann, D. J. and J. M. Rosen, Stratospheric sulfuric acid fraction and mass estimate for the 1982 volcanic eruption of El Chichon, Geophys. Res. Lett., 10, 313-316, 1983b.
- Hofmann, D. J. and J. M. Rosen, On the temporal variation of stratospheric aerosol size and mass during the first 18 months following the 1982 eruption of El Chichon, J. Geophys. Res., 89, 4883-4890, 1984.

Jager, H., R. Reiter, W. Carnuth and Sun Jian, Stratospheric aerosol layers during 1982 and 1983 as observed by lidar at Garmisch-Partenkirchen: 12th International Laser Radar Conference, Aix en Provence, France, August 13-17, 1984, Abstracts, pp. 207-210.

Kent, G. S. and M. P. McCormick, SAGE and SAM II measurements of global stratospheric aerosol optical depth and mass loading, J. Geophys. Res., 89, 5303-5313, 1984.

Kent, G. S., P. H. Wang, U. Farrukh and A. Deepak, Development of a global model for atmospheric backscatter at CO<sub>2</sub> wavelengths, Final Report on NASA Contract NAS8-35594, March, 1985.

Knollenberg, R. G. and D. Huffman, Measurements of the aerosol size distributions in the El Chichon cloud, Geophys. Res. Lett., 10, 1025-1028, 1983.

Krueger, A. J., Sighting of El Chichon sulfur dioxide clouds with the Nimbus 7 Total Ozone Mapping Spectrometer, Science, 23, 1983.

Labitzke, K., B. Naujokot and M. P. McCormick, Temperature effects on the stratosphere of the April 4, 1982 eruption of El Chichon, Mexico, Geophys. Res. Lett., 10, 24-26, 1983.

Lazrus, A. L., R. D. Cadle, B. W. Gandrud, J. P. Greenberg, B. J. Huebert, and W. I. Rose, Jr., Sulphur and halogen chemistry of the stratosphere and of volcanic eruption plumes, J. Geophys. Res., 84, 7869-7875, 1979.

McCormick, M. P. and T. J. Swissler, Stratospheric aerosol mass and latitudinal distribution of the El Chichon eruption cloud for October, 1982, Geophys. Res. Lett., 10, 877-880, 1983.

McCormick, M. P., T. J. Swissler, W. H. Fuller, W. H. Hunt and M. T. Osborn, Airborne and ground-based lidar measurements of the El Chichon stratospheric aerosol from 90°N to 56°S, Geof. Int., 23-2, 187-221, 1984.

McCormick, M. P., Lidar measurements of the El Chichon stratospheric aerosol climatology, 12th International Laser Radar Conference, Aix en Provence, France, August 13-17, 1984, Abstracts, pp. 207-210.

McCormick, M. P., El Chichon: Lidar and satellite measurements versus time and latitude, Topical Meeting of Optical Remote Sensing of the Atmosphere, January 15-18, 1985, Incline Village, Nevada, Technical Digest, pp. TuA2-1 to TuA2-5.

McCormick, M. P. and T. J. Swissler, Temporal variation and decay of the El Chichon stratospheric aerosol. [In preparation, 1985.]

Mauldin, L. E., N. H. Zaun, M. P. McCormick, J. H. Guy and W. R. Vaughn, Stratospheric Aerosol and Gas Experiment II instrument: A functional description, Opt. Eng., 24, 307-321, 1985.

Mroz, E. J., A. S. Mason and W. A. Sedlacek, Stratospheric sulfate from El Chichon and the mystery volcano, Geophys. Res. Lett., 10, 873-876, 1983.

- Oberbeck, V. R., E. F. Danielsen, K.G. Snetsinger and G. V. Ferry, Effect of the eruption of El Chichon on stratospheric aerosol size and composition, Geophys. Res. Lett., 10, 1021-1024, 1983.
- Post, M. J., Atmospheric infrared backscattering profiles: Interpretation of statistical and temporal properties, NOAA Technical Memorandum ERL WPL-122, May 1985.
- Reiter, R., H. Jager, W. Carnuth and W. Funk, The ElChichon cloud over central Europe, observed by lidar at Garmisch-Partenkirchen during 1982, Geophys. Res. Lett., 10, 1001-1004, 1983.
- Robock, A. and M. Matson, Circumglobal transport of the El Chichon volcanic dust cloud, Science, 22, 995-996, 1983.
- Shibata, T., M. Fujiwara and M. Hirono, The El Chichon volcanic cloud in the stratosphere: Lidar observations at Fukuoka and numerical simulation, J. Atmos. Terr. Phys., 46, 1121-1145, 1984.
- Spinhirne, J. D., El Chichon eruption cloud: Latitudinal variation of the spectral optical thickness for October 1982, Geophys. Res. Lett., 10, 881-884, 1983.
- Strong, A. E., Monitoring El Chichon aerosol distribution using NOAA-7 satellite AVHRR sea surface temperature observation, Geof. Int., (23-2), 129-142, 1984.
- Swissler, T. J., M. P. McCormick and J. D. Spinhirne, El Chichon eruption cloud, comparison of lidar and optical thickness measurements for October, 1982, Geophys. Res. Lett., 10, 885-888, 1983.
- Thomas, G. E., B. M. Jakosky, R. A. West and R. W. Sanders, Satellite limb-scanning thermal infrared observations of the El Chichon stratospheric aerosol: First results, Geophys. Res. Lett., 10, 997-1000.
- Turco, R. P., R. C. Whitten and O. B. Toon, Stratospheric aerosols: Observation and theory, Rev. of Geophys. and Space Physics, 20, 233-279, 1982.
- Uchino, O., On dispersion processes of the El Chichon dust particles in the lower stratosphere, J. Meteor. Soc. Japan, 63, 288-293, 1985.
- Vedder, J. F., E. P. Condon, E. C. Y. Inn, K. D. Tabor and M.A. Kritz, Measurements of stratospheric SO<sub>2</sub> after the El Chichon eruptions, Geophys. Res. Lett., 10, 1045-1048, 1983.
- Witteborn, F. C., K. O'Brien, H. W. Grean, J. B. Pollock, and K. H. Bilski, Spectroscopic measurements of the 8 - to 13-micrometer transmission of the upper atmosphere following the El Chichon eruptions, Geophys. Res. Lett., 10, 1009-1012, 1983.
- Woods, D. G. and R. L. Chuan, Size-specific composition of aerosols in the El Chichon volcanic cloud, Geophys. Res. Lett., 10, 1041-1044, 1983.